Centrifuge modeling of the impact of local and global scour erosion on the monotonic lateral response of a monopile in sand

Li, Q.; Prendergast, L. J.; Askarinejad, A.; Chortis, G.; Gavin, K.

DOI
10.1520/GTJ20180322

Publication date
2020

Document Version
Final published version

Published in
Geotechnical Testing Journal

ASTM INTERNATIONAL

Geotechnical Testing Journal

Q. Li,[1] L. J. Prendergast,[2] A. Askarinejad,[3] G. Chortis,[1] and K. Gavin[1]

DOI: 10.1520/GTJ20180322

Centrifuge Modeling of the Impact of Local and Global Scour Erosion on the Monotonic Lateral Response of a Monopile in Sand

Geotechnical Testing Journal

doi:10.1520/GTJ20180322 available online at www.astm.org

Q. Li,[1] L. J. Prendergast,[2] A. Askarinejad,[3] G. Chortis,[1] and K. Gavin[1]

Centrifuge Modeling of the Impact of Local and Global Scour Erosion on the Monotonic Lateral Response of a Monopile in Sand

Reference

Q. Li, L. J. Prendergast, A. Askarinejad, G. Chortis, and K. Gavin, "Centrifuge Modeling of the Impact of Local and Global Scour Erosion on the Monotonic Lateral Response of a Monopile in Sand," *Geotechnical Testing Journal* https://doi.org/10.1520/GTJ20180322

ABSTRACT

The majority of offshore wind turbines are founded on large-diameter, open-ended steel monopiles. Monopiles must resist lateral loads and overturning moments because of environmental (wind and wave) actions, whereas vertical loads tend to be comparatively small. Recent developments in turbine sizes and increases in hub heights have resulted in pile diameters increasing rapidly, whereas the embedment length to diameter ratio (L/D) is reducing. Soil erosion around piles, termed scour, changes the soil strength and stiffness properties and affects the system's load resistance characteristics. In practice, design scour depths of up to 1.3D are routinely assumed during the turbine lifetime; however, the impact on monopiles with low L/D is not yet fully understood. In this article, centrifuge tests are performed to assess the effect of scour on the performance of piles with low L/D. In particular, the effect of combined loads, scour type (global, local), and depth are considered. A loading system is developed that enables application of realistic load eccentricity and combined vertical, horizontal, and moment loading at the seabed level. An instrumented 1.8-m-diameter pile with $L/D = 5$ is used. A friction-reducing ball-type connection is designed to transfer lateral loads to the pile without inducing any rotational pile-head constraint, which is associated with loading rigs in tests of this nature. Results suggest that vertical and lateral load interaction is minimal. Scour has a significant impact on the lateral load-bearing capacity and stiffness of the pile, leads to increases in bending moment magnitude along the pile shaft, and lowers the location of peak pile bending moment. The response varies with scour type, with global scour resulting in larger moments than local scour. The size of the local scour hole is found to have a significant impact on the pile response, suggesting that scour hole width should be explicitly considered in design.

Manuscript received October 10, 2018; accepted for publication October 23, 2019; published online January 10, 2020.

[1] Department of Civil Engineering and Geosciences, Delft University of Technology, Building 23, Stevinweg 1, PO Box 5048, 2628 CN Delft / 2600 GA Delft, the Netherlands

[2] Department of Civil Engineering, Faculty of Engineering, University of Nottingham, Nottingham NG7 2RD, UK

[3] Department of Civil Engineering and Geosciences, Delft University of Technology, Building 23, Stevinweg 1, PO Box 5048, 2628 CN Delft / 2600 GA Delft, the Netherlands (Corresponding author), e-mail: A.Askarinejad@tudelft.nl, https://orcid.org/0000-0002-7060-2141

Keywords

centrifuge test, scour, monopile, lateral response

Introduction

The majority of offshore wind turbines (OWTs) constructed to date are founded on monopile foundations. Developments in construction methods and improved design procedures (Byrne et al. 2015a, 2018) have resulted in a gain in market share for monopiles from approximately 75 % of OWT foundations in 2012 (Doherty and Gavin 2012) to more than 87 % in 2017 (Wind Europe 2017). Monopiles are an efficient, cost effective, and proven technology to resist the large lateral loads and moments that are due to wind and wave actions, and thus provide a low-risk solution for offshore developers. Although all limit states are important, monopiles have strict serviceability requirements, e.g., total rotation at seabed level typically must remain less than 0.5° (Arany et al. 2017; Prendergast, Reale, and Gavin 2018).

When structures are founded in water, there is potential for erosion of the supporting soils, a mechanism known as scour. Interested readers are referred to Wang, Yu, and Liang (2017) for a comprehensive review on scour in the context of bridges. For the present application, scour erosion around unprotected offshore piles changes the support conditions and can pose a significant problem (Sørensen and Ibsen 2013; Prendergast, Gavin, and Doherty 2015). Scour increases the free cantilevered length of monopiles, leads to a reduction in the soil's effective stress, reducing the strength and stiffness of the remaining soil, and can thus compromise the serviceability and safety of structures (Hoffmans and Verheij 1997; Sumer and Fredsøe 2002). There are two main types of scour relevant to offshore structures, see **figure 1**: (i) 'global scour,' where the elevation of the soil surface is reduced globally because of natural sea bed migration or the presence of a whole wind farm interfering with the global flow regime, and (ii) 'local scour,' where the disturbed flow directly local to a pile structure leads to the formation of a conical scour pit around the foundation (Mostafa 2012). Global scour that is due to storm surge events has been reported in the literature (Robertson et al. 2007), with resulting scour depths of the order of $1D$(D = pile outer diameter). The typical range for local scour depth, D_s, considered in design is $1.3D$. It is noteworthy that in the marine environment, scour occurs because of the combination of tides, currents, and waves, which can make the estimation of scour depths very difficult (Prendergast, Gavin, and Doherty 2015; Negro et al. 2014). Because monopiles have slenderness ratios (pile penetration normalized by pile diameter, embedment length to diameter ratio [L/D]) of < 6, scour can have a major impact on the stiffness and capacity of these systems. Some previous works that have investigated the effect of scour on the lateral resistance characteristics of piles are discussed herein.

Bennett et al. (2009) examined the effect of scour and pile head boundary conditions on the lateral deflections of a pile group, used as the foundation for a bridge pier. The lateral behavior was examined using

FIG. 1

Schematic of local and global scour. w_b = bottom width of scour hole; w_t = top width of scour hole; α = scour slope angle; L = original embedment length; D = diameter; D_s = scour depth.

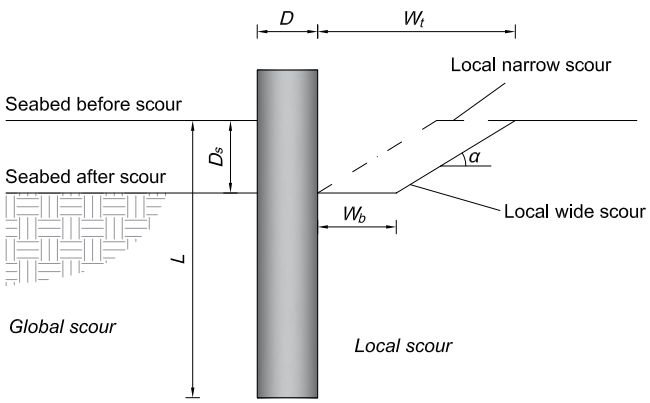

the Group Equivalent Pile method. Results showed that scour reduces the lateral capacity, which is especially significant when the scour depth exceeded the depth of the pile cap. Moreover, scour altered the influence depths of deflection, bending moment and shear, by lowering the point at which the maximum value of these parameters occurred. Lin et al. (2010) investigated the influence of the change in stress history of sand because of scour on the lateral behavior of piles by modifying soil reaction–lateral displacement (*p-y*) curves. They recognized that most scour analyses simply remove upper layers of soil to simulate scour with no change in the properties of the remaining soil, and this ignores the fact that the remaining soil will have experienced different stress histories before and after scour. By comparing calculated results from the modified sand *p-y* curves against a referenced field test, they concluded that the change in the overconsolidation ratio because of scour had the most significant influence on the sand lateral resistance properties, and leads to higher resistance in the remaining sand. Ignoring this additional effect is conservative. A subsequent study by the same authors in Lin et al. (2016) presents a simplified method for the analysis of laterally loaded piles in soft clay using modified *p-y* curves to account for scour hole dimensions (scour depth, scour width, scour-hole slope angle). By comparing the results of their model with a 3D finite difference model (developed using FLAC3D), it was observed that ignoring the scour hole dimensions could result in 10–19 % larger lateral displacement at the pile head with bending moments being 6–8 % larger, as compared to the case in which these are explicitly considered. Zhang, Chen, and Liang (2017) also recognized that soil stress history changes are typically ignored along with whole scour-hole geometry. They examined the behavior of laterally loaded long-slender piles ($L/D \approx 40$) in soft clay under scoured conditions by using modified *p-y* curves to reflect the effects of three-dimensional scour-hole geometry (depth, width, and slope angle) as well as the stress history of the soil. The results indicated that neglecting the effect of soil stress history can be unconservative for pile foundations in soft clay affected by scour. Furthermore, neglecting the scour-hole geometry is overconservative for design of laterally loaded piles under scour. For the purpose of design, the scour effect on the pile lateral behavior may be characterized in terms of scour depth and the stress history of the soil. Further work by the same authors extended this approach to investigate the influence of vertical loads on the lateral responses of scoured piles, taking soil stress history and scour hole geometry into consideration (Liang, Zhang, and Chen 2018). Mostafa (2012) investigated the influence of scour type (local and global) on the lateral response of piles in both cohesive and cohesionless soils using numerical modeling. The study concluded that scour had a more deleterious effect on piles installed in sand than in clay. In sand, scour depths ranging between 1*D* and 3*D* resulted in lateral pile head displacement increases of 37 to 155 %, as compared to the no scour condition. Moreover, global scour caused large increases in bending moments with the result that scour had a more significant impact for piles subjected to large lateral loads because of nonlinear pile-soil interaction effects. Qi et al. (2016) investigated the effect of scour type (local and global) on *p-y* curves of piles for OWTs in sand using centrifuge testing. They found that, under global scour, the *p-y* curves in the remaining overconsolidated soil showed no obvious difference to those in the original normally consolidated soil. This finding is contradictory to the hypothesis in Lin et al. (2010). Furthermore, under local scour, they found that the remaining overburden provided a beneficial response in that the lateral soil stiffness at a given depth below the scour hole base was greater than at the same relative depth below the original mudline. The tests were performed using relatively flexible piles with a slenderness ratio between 9.5 and 12.5.

To date, there has been considerable research undertaken on the effect of scour on the lateral response characteristics of piles using numerical modeling or scaled laboratory testing. Limited research has been undertaken, however, on the effect of scour depth and type on laterally loaded piles considering combined vertical, lateral, and moment loading at the seabed level using centrifuge testing, particularly for the piles with low slenderness ratios typically used for offshore wind developments. Moreover, the influence of local scour hole size has not received significant attention in physical modeling. This article presents the development of a centrifuge-based model specially designed to study the effect of scour on laterally loaded monopiles with low slenderness ratios. The challenge lies with the application of lateral loads and moments in a centrifuge while minimizing the constraint on the pile head fixity (i.e., the pile head should be free to rotate as per an offshore monopile).

Moreover, the presence of vertical dead loading representing the self-weight of an OWT should be considered. This article details the development of the testing arrangement in the Geo-Engineering laboratory at Delft University of Technology (TU Delft) and investigates lateral load-displacement responses and derived bending moment distributions of an instrumented pile under global scour and two types of local scour. The two types of local scour, termed narrow and wide in this article, refer to the bottom width of the scour hole, where $W_b = 0$ for narrow scour, and $W_b = D$ for wide scour (see fig. 1).

Centrifuge Modeling of Scoured Piles under Monotonic Lateral Loading

CENTRIFUGE FACILITY

The TU Delft centrifuge (see fig. 2) is a 2-m-diameter beam-type apparatus (Allersma 1994). Centrifuge tests are performed on models that are geometrically N-times smaller than a prototype. The geo-centrifuge provides a unique environment of enhanced gravitational acceleration (Ng), where the expected behavior of a full-scale geotechnical structure can be observed, with high precision, using small-scale models. The centrifuge at TU Delft enables models with dimensions up to 300 by 400 by 450 mm to be tested up to a maximum of 300 times the gravitational acceleration (300g). Although this is possible, for practical reasons related to the operation of the data logging equipment, samples are typically tested at a limiting gravitation acceleration of 100g.

For simulating geotechnical structures using a centrifuge, scaling laws must be considered. Table 1 provides a summary of typical scaling laws for modeling of pile-type structures. In this table, N refers to the gravitational acceleration field adopted in a given test.

FIG. 2 Schematic layout of the geo-centrifuge at TU Delft.

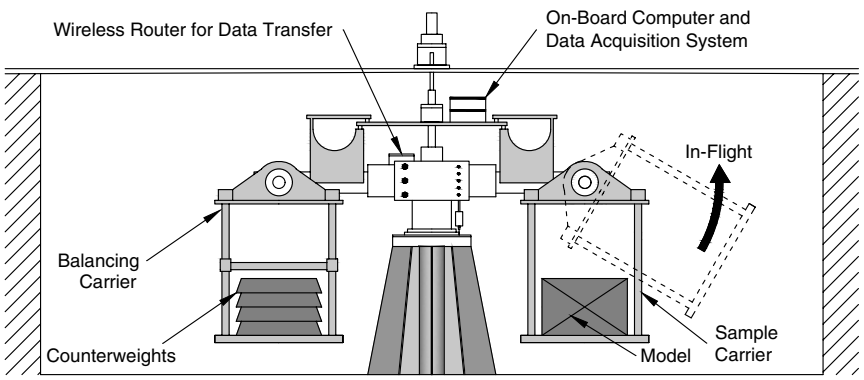

TABLE 1
Basic scaling laws for centrifuge modeling of monopiles

Term [Dimension]	Prototype	Model
Length (pile diameter, length) [L]	1	1/N
Second moment of area [L^4]	1	1/N^4
Flexural stiffness [ML^3/T^2]	1	1/N^4
Mass [M]	1	1/N^3
Force [ML/T^2]	1	1/N^2
Stress [$M/(LT^2)$]	1	1
Strain [−]	1	1

MODEL PILE

The model pile is an open-ended cylindrical aluminum tube with an outer diameter (D) of 18 mm (see **fig. 3**). The pile diameter is selected so as to minimize boundary effects associated with the strong box, which houses the pile, and also to satisfy constraints associated with the mean grain particle size (see the section "Soil Preparation and Characterization"). The strong box is fabricated from bolted plexiglas with dimensions 410 (length) by 150 (width) by 180 (height) mm^3 (see **figs. 4** and **5**). The pile has a total length of 240 mm and is embedded 90 mm into the sand. The embedded depth is chosen so as to model a pile with slenderness ratio (L/D) between 4–6 (Sørensen and Ibsen 2013; Doherty and Gavin 2012; LeBlanc, Houlsby, and Byrne 2010), within the typical range for offshore monopiles. A pile with embedded length of 90 mm equates to a slenderness ratio of 5. The wall thickness of the model pile is derived based on the calculations for minimum wall thickness for monopiles (API 2007; Arany et al. 2017). Using the similitude between the flexural rigidity (EI) of the prototype and the model (**Table 1**), the wall thickness is calculated to be 1 mm at model scale. Byrne et al. (2015b) have produced a database of piles, and they present the results of pile diameters normalized by pile wall thickness. For monopiles with $L/D = 5$, the value of D/t varied from 39 to 80. In the present analysis, the D/t value for the steel prototype pile is 60, which is within the expected range.

The pile was installed for each test by jacking in place at 1g prior to initiating the centrifuge. It should be noted that installing the model pile at 1g equates to an idealized 'wished-in-place' treatment, and it does not consider the potential residual base stresses that might be developed if driven while the centrifuge is in-flight. These residual stresses may lead to additional base moments on the piles (Murphy et al. 2018), which may alter the response characteristics. Moreover, installation of the pile at 1g results in shearing along the shaft at lower confining stresses compared to in-flight installation. This condition promotes dilative behavior of the sand at the shear band. However, because medium dense sand with a relative density (D_r) of 53 % is used in this study, significant dilative behavior is not expected. Furthermore, driving the pile at Ng would require stopping of

FIG. 3

Model pile schematic diagram with strain gage layout (dimensions in mm).

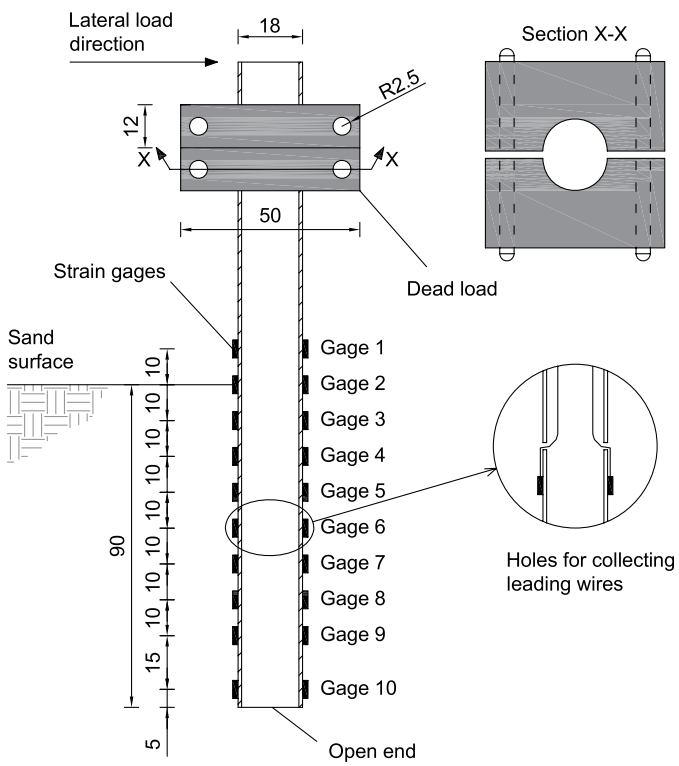

FIG. 4

Schematic of two-dimensional loading actuator and monopile arrangement in centrifuge tests.

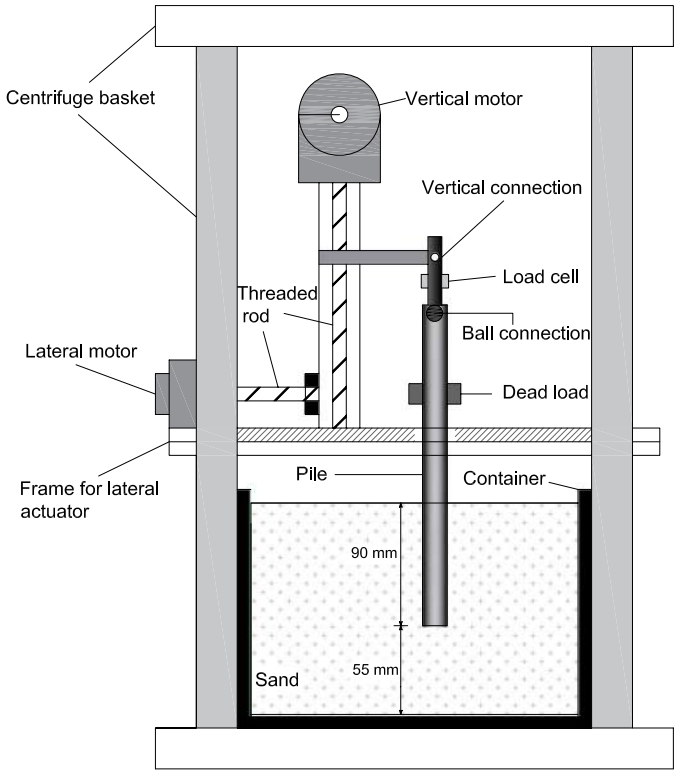

the centrifuge to adjust the loading rig for the subsequent lateral load application, which would add uncertainty surrounding the influence of the sample stress history on the results obtained. This article ignores the influence of installation effects.

All load tests were performed at 100*g*; therefore, the model pile properties correspond to a 1.8-m-diameter rigid structure with a wall thickness of 30 mm, an embedment of 9 m, and a total length of 24 m at the prototype scale. The primary dimensions and material properties of the pile are provided in **Table 2**.

Ten strain-gage pairs are installed along the pile shaft to enable derivation of the distribution of bending moments due to the applied loading. The strain gages used are FLA-3-11 fabricated by Tokyo Sokki Kenkyujo (Tokyo Sokki Kenkyujo 2018). Of these 10 gages, 7 may be logged simultaneously during testing because of a limitation in the available channels of the data acquisition system. In each analysis case conducted, the most appropriate seven gages are used. The load from the superstructure is incorporated by way of adding steel blocks with equivalent (prototype) weight of 3MN to the pile top. The masses were fabricated from quadrate steel with an outer length dimension of 50 mm and a thickness of 12 mm. In the center of each mass is a circular hole with a diameter of 18 mm to allow the masses to be fixed on the pile body (see **fig. 3**).

LOADING SYSTEM FOR PILE MODEL

The tests in this study were performed at 100*g* to model a rigid monopile with a diameter of 1.8 m (at prototype scale) and L/D of 5. A two-dimensional servo actuator applies loading to the pile head, as shown in **figures 4** and **5**. The loading system is capable of applying lateral loads under either load or displacement controlled conditions. The vertical dead load (V) at the pile head can be imposed by means of attaching steel blocks with different masses to model the presence of a superstructure (details of the dead load are described in the section "Model Pile"). The lateral load (L) is applied at the pile head by lateral movement of the actuator, and it is monitored by strain gages

FIG. 5

Picture of pile testing arrangement.

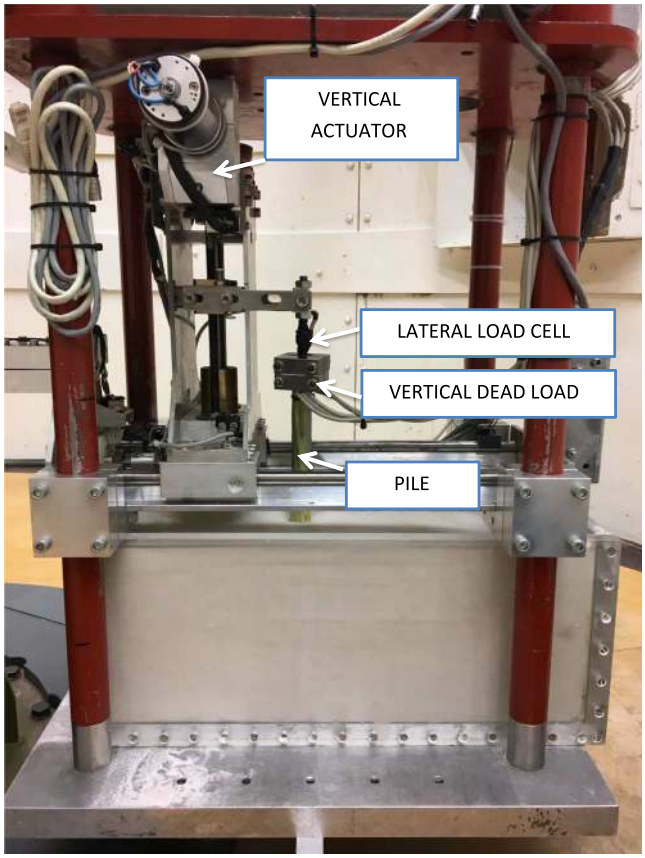

TABLE 2

Model and corresponding prototype pile dimensions and properties

Property	Model Pile	Prototype Pile[b]
Length (embedded + additional)	90 + 150 mm	9 + 15 m
Diameter, outer	18 mm	1.8 m
Wall thickness	1 mm	30 mm[a]
Young's modulus (E)	70 GPa	210 GPa[a]
Moment of inertia (I)	1,936 mm^4	0.065 m^4
Flexural stiffness (EI)	0.137 $kPa.m^4$	13.7 $GPa.m^4$

Note: [a] Assume prototype pile is fabricated from steel; [b] $N = 100$ adopted in the present study.

located on the loading arm. The lateral displacements of the pile at the loading position (pile head) can be monitored by the lateral motor encoders, the accuracy of which are of the order of approximately 3×10^{-5} mm. For all tests performed in this study, lateral loads are applied at a height of 15 m above the seabed at prototype scale.

Han and Frost (2000) recognized that the load-deflection response of a laterally loaded pile is highly dependent on the boundary conditions of the pile in the ground. Various boundary conditions for piles are encountered in practice, and four typical scenarios are shown in **figure 6**. Monopiles for OWTs will typically behave similarly to BC-4 (with some additional pile tip sway). Achieving the free head boundary condition in centrifuge

FIG. 6 Different boundary conditions for laterally loaded piles (after Han and Frost 2000): (*A*) head fixed against rotation with pile tip seated on hard soil; (*B*) head fixed against rotation with pile tip embedded in hard soil; (*C*) head free and pile tip embedded in hard soil; (*D*) head free with pile tip seated on hard soil. *L* = Lateral Load, *V* = Vertical Load.

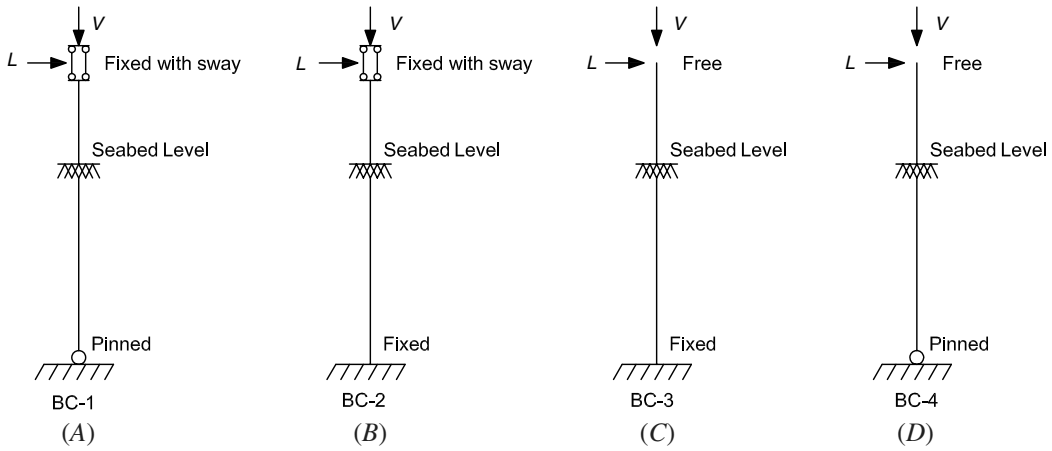

FIG. 7

Ball connection for reduced friction application of lateral load.

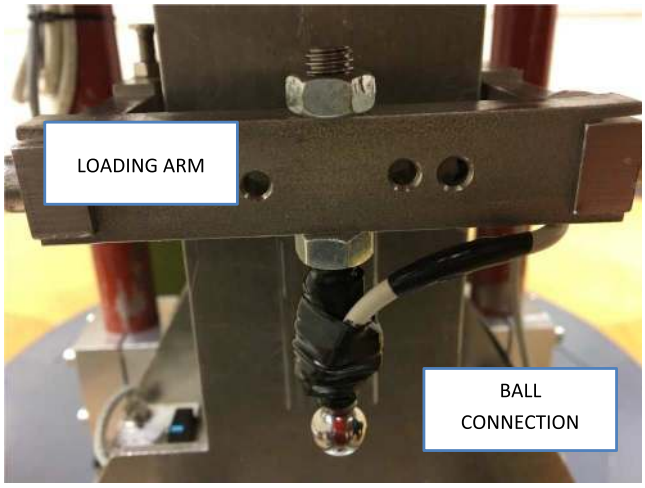

tests is difficult; therefore, most previous research tends to only consider lateral movement of the pile head (by implementing a roller-type connection) while ignoring any pile head rotation (BC-1 and BC-2).

To enable the application of a lateral load without inducing any rotational fixity associated with the loading arm, a specially designed friction-reducing ball connection (shown in **fig. 7**) was constructed to transfer the lateral loading produced by a linear actuator to the pile head. The ball is placed vertically into the open-end of the pile head, where it rests in contact with the internal shaft of the pile. A polytetrafluoroethylene sleeve is used to minimize the interface friction between the ball and the pile internal surface. **Figure 7** shows a photograph of the ball connection used in this study, and **figure 8** shows the instrumented model pile with polytetrafluoro-ethylene interior at the top and the shielded strain gages along the shaft.

SOIL PREPARATION AND CHARACTERIZATION

Fine, uniform Geba sand (SibelcoEurope 2016) was used in this study. It is mainly comprised of silica (99 % SiO_2), and 84.2 % of the grains have a diameter between 0.1 and 0.2 mm. The ratio of pile diameter to average grain size

FIG. 8

Pile with inner polytetrafluoroethylene material for reduced friction.

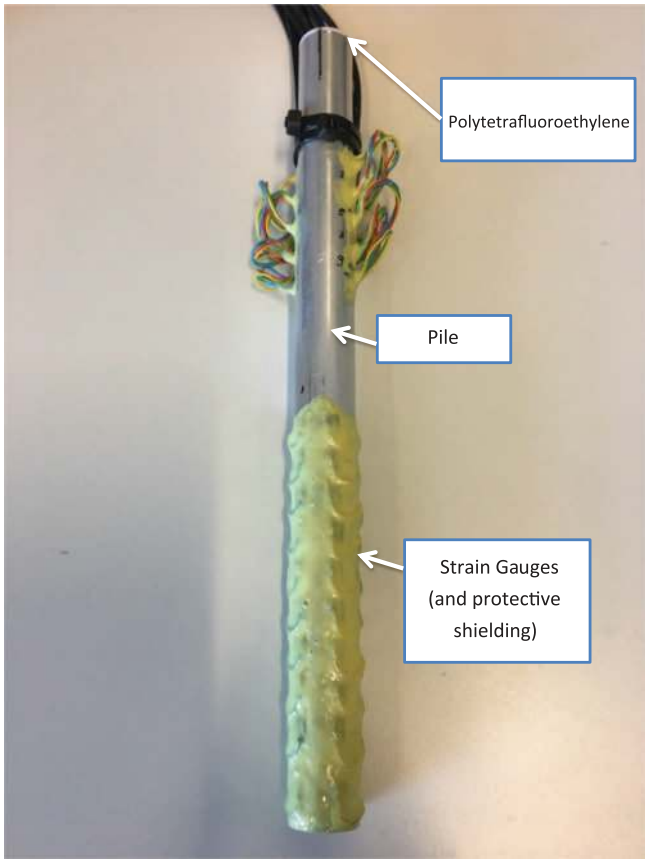

of the sands (D/D_{50}) for the tests is approximately 164, which is larger than the values of 20 and 60 suggested by Gui et al. (1998) and Remaud (1999), where grain size effects become negligible for laterally loaded piles (Garnier et al. 2007; Nunez, Hoadley, and Randolph 1988). A D_r of 53 % was adopted for the prepared sand used in the experiments conducted in this article. The main properties are summarized in **Table 3**. No water was considered in the experimental trials conducted in this article. It should be noted that although this is a simplification and a deviation from the physical reality of scoured offshore piles, the presence of water is not expected to alter the

TABLE 3

Basic soil properties of Geba sand (De Jager et al. 2017; Maghsoudloo et al. 2018)

Property	Sand
Group symbol based on USCS[a]	SP
Median particle size, D_{50} (mm)	0.11
Curvature coefficient, C_C	1.24
Uniformity coefficient, C_U	1.55
Specific gravity, G_S	2.67
Plasticity index, *PI*	NP
Maximum void ratio, e_{max}	1.07
Minimum void ratio, e_{min}	0.64

Note: [a] Unified Soil Classification System (USCS) (ASTM D2487).

observed behavioral trends, rather its presence would lower the effective unit weight of the sand. A similar treatment can be observed in Mu et al. (2018); Verdure, Garnier, and Levacher (2003); Klinkvort and Hededal (2013); LeBlanc, Houlsby, and Byrne (2010); and Li, Haigh, and Bolton (2010).

SCOUR HOLE EXCAVATION

In order to study the effect of different types of scour erosion, it is necessary to develop a method to model scour hole geometries in the centrifuge. To cover the main range of expected scour hole geometries, three different scour hole shapes (one for global scour and two for local scour) were considered (see **fig. 1**). **Figure 1** shows a schematic of simplified global and local scour. In the models, D denotes pile diameter, W_t denotes top width of scour hole, W_b denotes bottom width of scour hole, D_s denotes scour depth, and α denotes slope angle of the scour hole. A range of scour depths of 1D, 1.5D, and 2D were implemented in this study to cover the ranges considered by Kishore, Rao, and Mani (2008); Sumer, Fredsøe, and Christiansen (1992); Sumer, Hatipoglu, Fredsøe (2007); and Det Norske Veritas (2014). Global scour was modeled through the complete removal of a given soil layer (see **fig. 1**) and typically occurs because of natural seabed migration. Local scour represents the case of a scour hole forming in the direct vicinity of a pile. To model local scour, a scour hole was created in the shape of an inverted frustum. To investigate the influence of scour hole size, the scour hole base extends around the pile at a distance (W_b) varying between 0 and D. A scour hole with a base width $W_b = 0$ is termed "local narrow scour," whereas a scour hole with a base width $W_b = D$ is termed "local wide scour" in subsequent analyses in this article. A scour hole side slope of 30° was adopted for all cases, which is in line with previous experiments (Roulund et al. 2005; Hoffmans and Verheij 1997). Note, the scour side slope angle is the least important factor among the three scour hole dimensions (scour depth, scour width, scour-hole slope angle) influencing the responses of laterally loaded piles (Li, Han, and Lin 2013; Zhang, Chen, and Liang 2017). For this reason, it is kept constant in this study.

To excavate sand to form the scour hole types described, rigid molds were fabricated, as shown schematically in **figure 9**. These molds, with varying depths and base widths, were used to ensure the shape of the scour holes adhered to the required dimensions for each test. Each scour hole was created immediately prior to jacking the model pile at 1g and just before spinning the centrifuge up to 100g.

TESTING PROGRAM

Displacement-controlled lateral loading is applied to the pile head by the lateral movement of the actuator at a constant displacement rate of 0.01 mm/s. Each test continues until the loading arm reaches the target displacement. The testing program comprised investigating the effect of scour depth and scour type on the lateral behavior of the pile (capacity and bending moment). No scour, and three scour depths equating to 1D, 1.5D, and 2D, were studied. Moreover, three scour types, namely local narrow scour, local wide scour, and global scour were also investigated to ascertain the influence of scour hole size (overburden dependency) on the pile lateral behavior. Each test was undertaken twice to ensure repeatability. A constant vertical load of 3MN was applied to represent the weight of a superstructure. The testing program is summarized in **Table 4**.

FIG. 9

Schematics of (*A*) scour hole molds of local narrow scour and (*B*) scour hole molds of local wide scour.

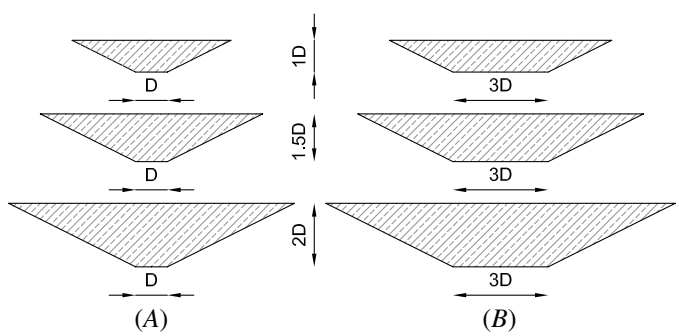

TABLE 4
Program of centrifuge test

Test Number	Scour Type	Scour Depth	Vertical Dead Load at Prototype Scale (MN)	Description
1	No scour	…	0, 1.5, and 3	Zero scour lateral load test
2	Global scour	1D	3	Scour test
3	Global scour	1.5D	3	Scour test
4	Global scour	2D	3	Scour test
5	Local wide scour	1D	3	Scour test
6	Local wide scour	1.5D	3	Scour test
7	Local wide scour	2D	3	Scour test
8	Local narrow scour	1D	3	Scour test
9	Local narrow scour	1.5D	3	Scour test
10	Local narrow scour	2D	3	Scour test

Results and Discussion

The load-displacement response and bending moment profiles of the piles under various scour conditions are reported in this section.

LATERAL LOAD-DISPLACEMENT AND BENDING MOMENTS UNDER ZERO SCOUR CONDITION

The pile head load-displacement response measured for the no-scour base-case condition is shown in figure 10 (Test 1). The ultimate lateral resistance of a pile is usually defined as a displacement equal to 10 % of the pile diameter, $H_{0.1}$, at the seabed (mudline) level. In this study, the pile head displacement (as opposed to the seabed displacement), is the measured parameter, which is 15 m above the seabed level (at the prototype scale). For the purpose of comparison of the scour cases considered in this article, the ultimate resistance, H_{ult}, is defined as a pile head displacement of 1 pile diameter, in this case 1.8 m. In figure 10, the pile is loaded up to and beyond the specified ultimate resistance, and it can be seen that the lateral resistance continues to increase to a value of 970 kN at a lateral pile-head displacement of 3 m (fig. 10*A*). The presence of a vertical load (superstructure weight) had a minimal effect on the lateral response for this pile geometry with the H_{ult} capacity changing by approximately 1 % as the vertical applied load increased from 0 to 3 MN. As a result, all remaining tests were performed with a 3 MN vertical load to represent the superstructure weight.

Figure 10*B* shows the bending moments derived from the strain gage readings using 7 of the 10 strain gage pairs for the applied loading in figure 10*A*. As discussed earlier, because of limitations with the data logger, only seven strain gage pairs could be analyzed at any one time. Bending moments are derived from bending strain measurements using equation (1).

$$M(z) = EI\rho(z) \tag{1}$$

where EI is the flexural rigidity of the pile and $\rho(z)$ is the curvature at a given applied load, obtained as the ratio between the difference in measured compressive and tensile strains to the gage lever arm (pile diameter) at a given depth z. The absolute values of the bending moments derived from each of the strain gages show an increasing trend with increased lateral displacement. In order to understand the evolution in the relative magnitudes of these bending moments along the pile, these are better viewed by plotting the values of bending moment at a given depth along the pile as a function of the pile head displacement. This is undertaken in figure 10*C*, which shows the evolution in bending moment profiles along the pile as the lateral pile head deflection (h) increased from 0.5 to 3 m. As is evident, the shape of the bending moment profile is broadly conserved for increasing pile displacements, and the peak bending moment occurs at approximately the same depth in each case (between −2 and −3 m below ground level [bgl]).

FIG. 10 Zero scour response features from centrifuge testing at prototype scale: (*A*) pile head lateral load-displacement response, (*B*) bending moment measurements along the pile, (*C*) bending moment profiles for different levels of pile head displacement (*h*).

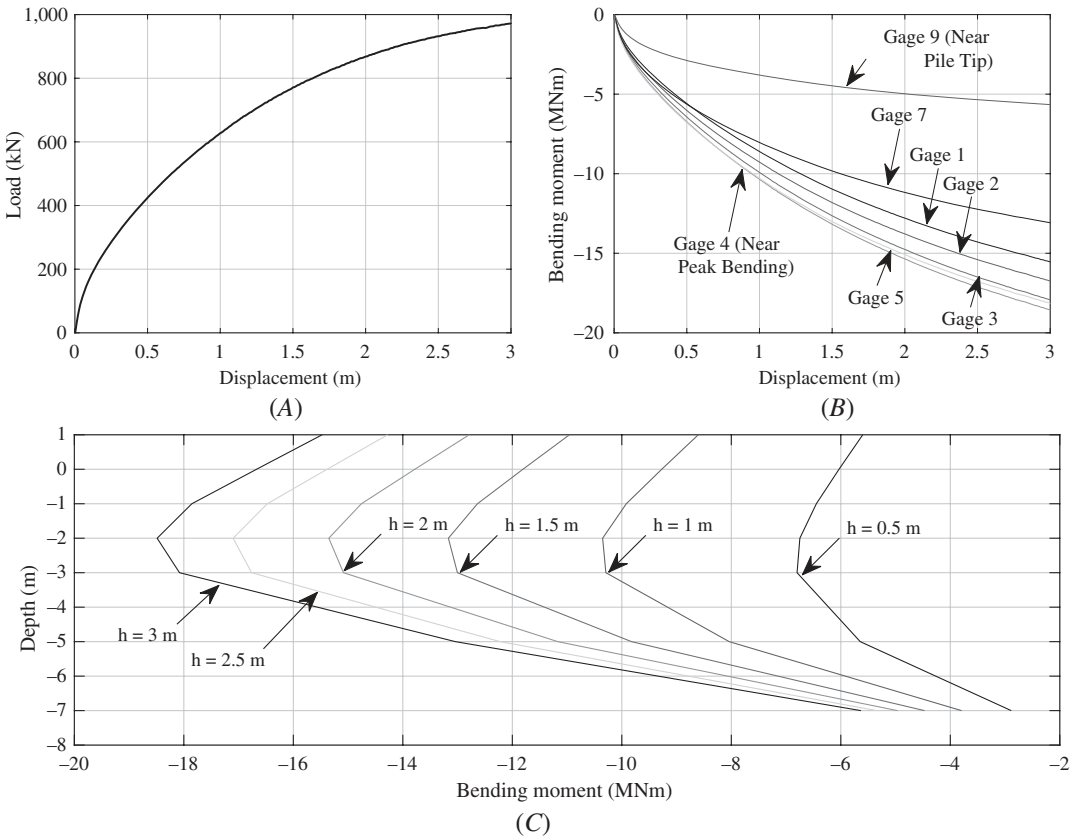

EFFECT OF SCOUR DEPTH ON THE LATERAL PILE RESPONSE

The impact of four different local scour depths are investigated in this section, namely zero scour and scour with depths 1*D*, 1.5*D*, and 2*D*. Only the results for a single scour type, namely local wide scour, are considered. For this scour hole type, sand is removed up to a distance of 1*D* from around the pile. The influence of scour size is investigated in a subsequent section.

The impact of increasing scour depth on the pile head lateral load-displacement responses is shown in **figure 11*A***. For the cases considered, the H_{ult} value reduces from 831 to 234 kN as the scour depth increases to 2*D*, a reduction of almost 72 %. This result corroborates the findings in Lin et al. (2016), which stated that scour depth is the most critical factor influencing the lateral behavior of piles.

The bending moment distributions under 0, 1*D*, 1.5*D*, and 2*D* scour are reported in **figure 11*B*** for an applied lateral pile head load of 100 kN. As the scour depth increases, the absolute value of the maximum bending moment (M_{max}) increases from 1.527 MNm for zero scour, to 1.615 MNm for 1*D* scour, to 1.711 MNm for 1.5*D* scour, to 1.86 MNm for 2*D* scour. This represents a change in peak bending moment of 5.8 %, 12.1 %, and 21.8 % relative to the no scour case for 1*D*, 1.5*D*, and 2*D* scour, respectively. Furthermore, the location of the M_{max} also moves progressively down the pile as scour depth increases, moving from −3 m bgl to −5 m bgl. These findings are in line with previous research (Bennett et al. 2009), where the influence depth is observed to increase.

FIG. 11 Effect of scour depth on pile response characteristics at prototype scale: (*A*) lateral load-displacement response under increasing local wide scour, (*B*) bending moment derived from strains for increasing scour.

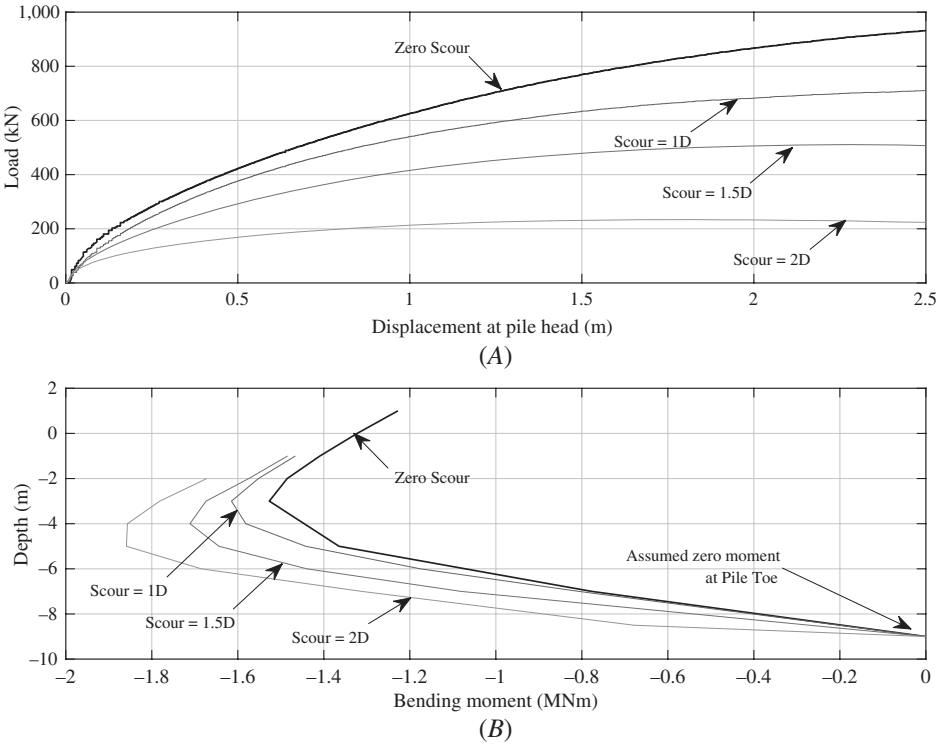

EFFECT OF SCOUR TYPE ON THE PILE LATERAL RESPONSE

In this section, the effect of the scour type on the bending moment distribution along the pile under scour is investigated. Local narrow, local wide, and global scour types are compared with a view to ascertaining if the scour hole size and associated overburden influence has an effect on the resulting bending moment distribution. **Figure 12*A*** shows the bending moment distribution measured along the pile under a scour depth of 1*D* for the three scour types because of an applied lateral load of 100 kN at the pile head. Similar to that shown previously, the absolute value of the bending moment profile increases between zero scour and 1*D* scour. Evidently, there is a difference between the local scour and global scour bending moment profiles in that the global scour profile results in larger absolute values of bending moment under the applied load than the local scour profiles. For the scour depth of 1*D* (**fig. 12*A***), both local narrow and local wide scour exhibit similar bending moment profiles, suggesting that for this scour depth, there is a negligible difference that is due to the variation in overburden pressure between both local scour widths. The M_{max} increases 5.8 % from the no scour case to the local scour cases and 10.7 % from the no scour case to the global scour case. It is interesting to note that the percentage change in the peak bending moment between no scour and global scour for a depth of 1*D* (10.7 %, **fig. 12*A***) is almost the same as the percentage change from no scour to local wide scour with a depth of 1.5*D*(12.1 %, **fig. 11*B***), as discussed in the section "Effect of Scour Depth on the Lateral Pile Response." Although scour depth is still the most influential factor for laterally loaded piles, this finding suggests that the overburden influence is quite important nonetheless. The location of the point of maximum moment reduces from −3 to −4 m bgl, which suggests that the additional loss in overburden for the case of global scour relative to local scour forces the pile to mobilize resistance from a deeper depth of soil, in order to compensate for the loss of strength of the remaining soil.

FIG. 12

Effect of scour type on bending moments measured along pile for applied lateral load = 100 kN, at prototype scale: (*A*) bending moments for narrow, wide, and global scour to depth 1*D*; (*B*) bending moments for narrow, wide, and global scour to depth 2*D*.

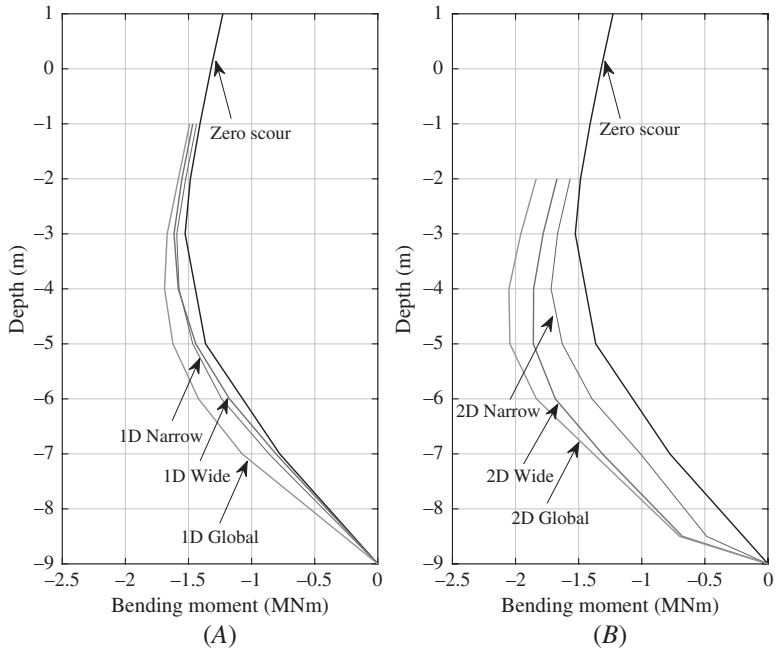

Figure 12*B* shows the same information as **figure 12*A***, but for a scour depth of 2*D*. In this case, there is a clear increase in the absolute magnitude of the bending moment profiles measured between no scour and the three scour types. This suggests that soil close to the pile in the narrow scour case provides enhanced effective confining stiffness because of the presence of the remaining overburden. M_{max} increases 12.5 % from the no scour to local narrow scour case, 21.7 % to the local wide scour case, and 34.4 % to the global scour case. The location of the point of maximum moment reduces from −3 to −5 m below seabed level, as the soil seeks to balance the external loads by mobilizing deeper soils to compensate for the overburden differences as discussed previously. The influence of scour hole width is a significant finding because many previous researchers completely ignored this effect and simplified scour as the increase in free length of a structural element without paying due attention to the properties of the remaining soil (Li et al. 2017; Prendergast, Hester, and Gavin 2016). The physical modeling results in this article highlight that this influence should not be discounted.

Conclusions

This article presents the development of a specially designed pile lateral loading system for centrifuge model tests that minimizes the pile-head rotational constraint associated with tests of this nature. A modeling scheme to evaluate lateral pile behavior under combined lateral and moment loading at the seabed level, under various scour conditions, is undertaken using this ball-type loading system. The research is applicable to offshore monopiles that have low slenderness ratios and that are used to support wind turbines. The study has several conclusions:

- The friction-reducing ball connection with a polytetrafluoroethylene interface is adept at providing a lateral monotonic load with significantly reduced pile-head rotational fixity. This is useful for research on offshore monopile models, which have a free head condition. Other types of loading rigs that use pin-type connections have a tendency to apply a component of vertical loading to pile models as lateral displacements become large. The ball-type connection adopted in this study mitigates this issue.

- Scour reduces the lateral bearing capacity and stiffness of pile foundations and leads to increased bending moments along the pile under similar lateral loads applied at the pile head. Moreover, the location of the M_{max} occurs lower along the pile for increased scour, which may have implications for the design of monopiles with variable wall thickness. Increased pile wall thickness may be adopted in the region near surface soils to increase bending resistance locally; therefore, changes in the response regime that are due to scour have potential design ramifications and should be considered.
- In addition to scour reducing lateral capacity, the width of the scour hole has a noticeable effect on the measured bending moments. For a scour depth of 1*D*, there is a distinct increase in the bending moments for the case of global scour compared to local scour. However, little difference is observed between both local narrow and local wide scour at this scour depth. For the case of scour up to a depth of 2*D*, however, there is a significant difference between the bending moments measured for each scour type, with the bending moment consistently increasing from the no scour case to local narrow scour, to local wide scour, and on to global scour. This finding suggests that designers should explicitly consider scour hole geometry in design (at least in a preliminary capacity) because it is conservative to assume the entire soil layer is removed during scour. For local scour, the overburden close to the pile provides additional resistance to the remaining soil, reducing the bending moments relative to global scour.

This article presented the background to the centrifuge-based analysis regime for a pile under various scour conditions. It should be noted that installation effects were not considered because the model piles were jacked into the soil at 1*g* prior to testing. If the piles were driven while in-flight, this would lead to the generation of residual base stresses and potential moments at the pile base. Although the analysis in this article does not consider the presence of these additional base moments, the behavioral trends identified in this article should not be affected. Further studies will expand the investigation to the influence of scour on soil reaction-lateral displacement *p-y* curves for piles with low slenderness ratios.

ACKNOWLEDGMENTS

This work is partly funded by the Section of Geo-Engineering of Delft University of Technology, EU Horizon 2020 SAFE-10-T Project No. 723254 (supported the second author) and the China Scholarship Council (supported the first author). Moreover, the second author wishes to acknowledge the Faculty of Engineering, University of Nottingham, for financial support received to facilitate this collaboration.

References

Allersma, H. G. B. 1994. "The University of Delft Geotechnical Centrifuge." In *Centrifuge 94*, 47–52. Rotterdam, the Netherlands: A. A. Balkema.

API. 2007. *RP2A: Recommended Practice for Planning, Designing and Constructing Offshore Platforms - Working Stress Design*. Washington, DC: American Petroleum Institute.

Arany, L., S. Bhattacharya, J. Macdonald, and S. J. Hogan. 2017. "Design of Monopiles for Offshore Wind Turbines in 10 Steps." *Soil Dynamics and Earthquake Engineering* 92 (January): 126–152. https://doi.org/10.1016/j.soildyn.2016.09.024

Bennett, C. R., C. Lin, R. Parsons, and J. Han. 2009. "Evaluation of Behavior of a Laterally Loaded Bridge Pile Group under Scour Conditions." In *Structures Congress 2009: Don't Mess with Structural Engineers: Expanding Our Role*. Reston, VA: American Society of Civil Engineers.

Byrne, T., K. Gavin, L. J. Prendergast, P. Cachim, P. Doherty, and S. Chenicheri Pulukul. 2018. "Performance of CPT-Based Methods to Assess Monopile Driveability in North Sea Sands." *Ocean Engineering* 166 (October): 76–91. https://doi.org/10.1016/j.oceaneng.2018.08.010

Byrne, B. W., R. McAdam, H. Burd, G. T. Houlsby, C. M. Martin, L. Zdravković, D. M. Taborda, et al. 2015a. "New Design Methods for Large Diameter Piles under Lateral Loading for Offshore Wind Applications." In *International Symposium on Frontiers in Offshore Geotechnics*, 705–710. Reston, VA: Geo-Institute.

Byrne, B. W., R. A. McAdam, H. J. Burd, G. T. Houlsby, C. M. Martin, K. Gavin, P. Doherty, et al. 2015b. "Field Testing of Large Diameter Piles under Lateral Loading for Offshore Wind Applications." In *Proceedings of the XVI ECSMGE Geotechnical Engineering for Infrastructure and Development*, 1255–1260. London: Institution of Civil Engineers.

De Jager, R. R., A. Maghsoudloo, A. Askarinejad, and F. Molenkamp. 2017. "Preliminary Results of Instrumented Laboratory Flow Slides." In *First International Conference on the Material Point Method*. Delft, the Netherlands: Elsevier Ltd.

Det Norske Veritas. 2014. *DNV Offshore Standard DNV-OS-J101 Design of Offshore Wind Turbine Structures*. DNV-OS-J101. Bærum, Norway: Det Norske Veritas, May 2014.

Doherty, P. and K. Gavin. 2012. "Laterally Loaded Monopile Design for Offshore Wind Farms." *Proceedings of the Institution of Civil Engineers - Energy* 165, no. 1 (February): 7–17. https://doi.org/10.1680/ener.11.00003

Garnier, J., C. Gaudin, S. M. Springman, P. J. Culligan, D. Goodings, D. Konig, B. Kutter, R. Phillips, M. F. Randolph, and L. Thorel. 2007. "Catalogue of Scaling Laws and Similitude Questions in Geotechnical Centrifuge Modelling." *International Journal of Physical Modelling in Geotechnics* 7, no. 3 (September): 1–23. https://doi.org/10.1680/ijpmg.2007.070301

Gui, M., M. Bolton, J. Garnier, J. Corte, G. Bagge, J. Laue, and R. Renzi. 1998. "Guidelines for Cone Penetration Tests in Sand." *Centrifuge 98: International Conference*, 155–160. London: Taylor and Francis.

Han, J. and J. D. Frost. 2000. "Load–Deflection Response of Transversely Isotropic Piles under Lateral Loads." *International Journal for Numerical and Analytical Methods in Geomechanics* 24, no. 5 (April): 509–529. https://doi.org/10.1002/(SICI)1096-9853(20000425)24:5<509::AID-NAG79>3.0.CO;2-9

Hoffmans, G. J. and H. J. Verheij. 1997. *Scour Manual*. Boca Raton, FL: CRC Press.

Kishore, Y. N., S. N. Rao, and J. Mani. 2008. "Influence of the Scour on Laterally Loaded Piles." In *The 12th International Conference of International Association for Computer Methods and Advances in Geomechanics*. Red Hook, NY: Curran.

Klinkvort, R. T. and O. Hededal. 2013. "Lateral Response of Monopile Supporting an Offshore Wind Turbine." *Proceedings of the Institution of Civil Engineers - Geotechnical Engineering* 166, no. 2: 147–158. https://doi.org/10.1680/geng.12.00033

LeBlanc, C., G. T. Houlsby, and B. W. Byrne. 2010. "Response of Stiff Piles in Sand to Long-Term Cyclic Lateral Loading." *Géotechnique* 60, no. 2 (February): 79–90. https://doi.org/10.1680/geot.7.00196

Li, F., J. Han, and C. Lin. 2013. "Effect of Scour on the Behavior of Laterally Loaded Single Piles in Marine Clay." *Marine Georesources & Geotechnology* 31, no. 3: 271–289. https://doi.org/10.1080/1064119X.2012.676157

Li, S., S. He, H. Li, and Y. Jin. 2017. "Scour Depth Determination of Bridge Piers Based on Time-Varying Modal Parameters: Application to Hangzhou Bay Bridge." *Journal of Bridge Engineering* 22, no. 12 (December): 1–13. https://doi.org/10.1061/(ASCE)BE.1943-5592.0001154

Li, Z., S. K. Haigh, and M. D. Bolton. 2010. "Centrifuge Modelling of Mono-Pile under Cyclic Lateral Loads." In *Seventh International Conference on Physical Modelling in Geotechnics*, 965–970. Boca Raton, FL: CRC Press.

Liang, F., H. Zhang, and S. Chen. 2018. "Effect of Vertical Load on the Lateral Response of Offshore Piles Considering Scour-Hole Geometry and Stress History in Marine Clay." *Ocean Engineering* 158 (June): 64–77. https://doi.org/10.1016/j.oceaneng.2018.03.070

Lin, C., C. Bennett, J. Han, and R. L. Parsons. 2010. "Scour Effects on the Response of Laterally Loaded Piles Considering Stress History of Sand." *Computers and Geotechnics* 37, no. 7 (November): 1008–1014. https://doi.org/10.1016/j.compgeo.2010.08.009

Lin, C., J. Han, C. Bennett, and R. L. Parsons. 2016. "Analysis of Laterally Loaded Piles in Soft Clay Considering Scour-Hole Dimensions." *Ocean Engineering* 111 (January): 461–470. https://doi.org/10.1016/j.oceaneng.2015.11.029

Maghsoudloo, A., A. Askarinejad, R. R. De Jager, F. Molenkamp, and M. A. Hicks. 2018. "Experimental Investigation of Pore Pressure and Acceleration Development in Static Liquefaction Induced Failures in Submerged Slopes." In *Ninth International Conference of Physical Modelling in Geotechnics*. London: Taylor and Francis.

Mostafa, Y. E. 2012. "Effect of Local and Global Scour on Lateral Response of Single Piles in Different Soil Conditions." *Engineering* 4: 297–306. https://doi.org/10.4236/eng.2012.46039

Mu, L., X. Kang, K. Feng, M. Huang, and J. Cao. 2018. "Influence of Vertical Loads on Lateral Behaviour of Monopiles in Sand." *European Journal of Environmental and Civil Engineering* 22, no. sup1: 286–301. https://doi.org/10.1080/19648189.2017.1359112

Murphy, G., D. Igoe, P. Doherty, and K. Gavin. 2018. "3D FEM Approach for Laterally Loaded Monopile Design." *Computers and Geotechnics* 100 (August): 76–83. https://doi.org/10.1016/j.compgeo.2018.03.013

Negro, V., J.-S. López-Gutiérrez, M. D. Esteban, and C. Matutano. 2014. "Uncertainties in the Design of Support Structures and Foundations for Offshore Wind Turbines." *Renewable Energy* 63 (March): 125–132. https://doi.org/10.1016/j.renene.2013.08.041

Nunez, I. L., P. J. Hoadley, and M. F. Randolph. 1988. "Driving and Tension Loading of Piles in Sand on a Centrifuge." In *Proceedings of the International Conference Centrifuge*, 353–362. Rotterdam, the Netherlands: A. A. Balkema.

Sørensen, S. P. H. and L. B. Ibsen. 2013. "Assessment of Foundation Design for Offshore Monopiles Unprotected against Scour." *Ocean Engineering* 63 (May): 17–25. https://doi.org/10.1016/j.oceaneng.2013.01.016

Prendergast, L. J., K. Gavin, and P. Doherty. 2015. "An Investigation into the Effect of Scour on the Natural Frequency of an Offshore Wind Turbine." *Ocean Engineering* 101 (June): 1–11. https://doi.org/10.1016/j.oceaneng.2015.04.017

Prendergast, L. J., D. Hester, and K. Gavin. 2016. "Determining the Presence of Scour around Bridge Foundations Using Vehicle-Induced Vibrations." *Journal of Bridge Engineering* 21, no. 10 (October): 1–14. https://doi.org/10.1061/(ASCE)BE.1943-5592.0000931

Prendergast, L. J., C. Reale, and K. Gavin. 2018. "Probabilistic Examination of the Change in Eigenfrequencies of an Offshore Wind Turbine under Progressive Scour Incorporating Soil Spatial Variability." *Marine Structures* 57 (January): 87–104. https://doi.org/10.1016/j.marstruc.2017.09.009

Qi, W. G., F. P. Gao, M. F. Randolph, and B. M. Lehane. 2016. "Scour Effects on p–y Curves for Shallowly Embedded Piles in Sand." *Géotechnique* 66, no. 8 (August): 648–660. https://doi.org/10.1680/jgeot.15.P.157

Remaud, D. 1999. "Pieux Sous Charges Latérales: Étude Expérimentale de l'effet de Groupe [Piles under Lateral Loads: Experimental Study of the Group Effect]." Nantes, France: Ecole Centrale de Nantes.

Robertson, I. N., H. R. Riggs, S. C. S. Yim, and Y. L. Young. 2007. "Lessons from Hurricane Katrina Storm Surge on Bridges and Buildings." *Journal of Waterway, Port, Coastal, and Ocean Engineering* 133, no. 6 (November/December): 463–483. https://doi.org/10.1061/(ASCE)0733-950X(2007)133:6(463)

Roulund, A., B. M. Sumer, J. Fredsøe, and J. Michelsen. 2005. "Numerical and Experimental Investigation of Flow and Scour around a Circular Pile." *Journal of Fluid Mechanics* 534 (July): 351–401. https://doi.org/10.1017/S0022112005004507

SibelcoEurope. 2016. "Technical Data: Geba Sand." Eurogrit BV.

Sumer, B. M. and J. Fredsøe. 2002. *The Mechanics of Scour in the Marine Environment*. Hackensack, NJ: World Scientific.

Sumer, B. M., F. Hatipoglu, and J. Fredsøe. 2007. "Wave Scour around a Pile in Sand, Medium Dense, and Dense Silt." *Journal of Waterway, Port, Coastal, and Ocean Engineering* 133, no. 1 (January): 14–27. https://doi.org/10.1061/(ASCE)0733-950X(2007)133:1(14)

Sumer, B. M., J. Fredsøe, and N. Christiansen. 1992. "Scour around Vertical Pile in Waves." *Journal of Waterway, Port, Coastal and Ocean Engineering* 118, no. 1 (January): 15–31. https://doi.org/10.1061/(ASCE)0733-950X(1992)118:1(15)

Tokyo Sokki Kenkyujo. 2018. "Strain Gauge Product Information." 2018. http://web.archive.org/web/20190731182929/https://tml.jp/e/product/strain_gauge

Verdure, L., J. Garnier, and D. Levacher. 2003. "Lateral Cyclic Loading of Single Piles in Sand." *International Journal of Physical Modelling in Geotechnics* 3, no. 3 (September): 17–28. https://doi.org/10.1680/ijpmg.2003.030303

Wang, C., X. Yu, and F. Liang. 2017. "A Review of Bridge Scour: Mechanism, Estimation, Monitoring and Countermeasures." *Natural Hazards* 87, no. 3 (July): 1881–1906. https://doi.org/10.1007/s11069-017-2842-2

Wind Europe. 2017. *Offshore Wind in Europe - Key Trends and Statistics*. Brussels, Belgium: WindEurope.

Zhang, H., S. Chen, and F. Liang. 2017. "Effects of Scour-Hole Dimensions and Soil Stress History on the Behavior of Laterally Loaded Piles in Soft Clay under Scour Conditions." *Computers and Geotechnics* 84 (April): 198–209. https://doi.org/10.1016/j.compgeo.2016.12.008